Analytical Methods

Accepted Manuscript

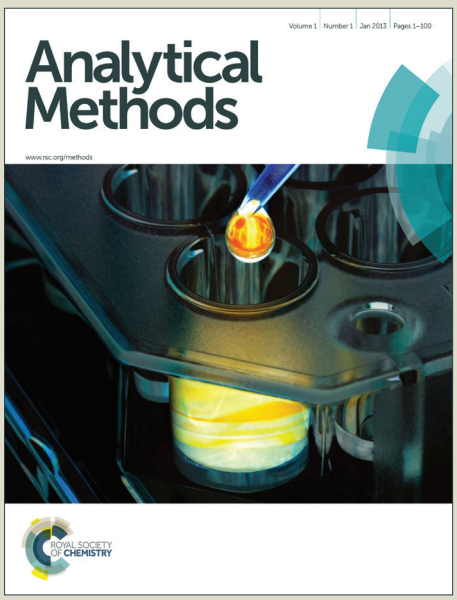

ROYAL SOCIETY OF CHEMISTRY

www.rsc.org/methods

Mussel inspired redox surface for one step visual and colorimetric detection of Hg^{2+} during the formation of Ag@DOPA@Hg nanoparticles

Yuling Hu, Dongmei Wang and Gongke Li**

School of Chemistry and Chemical Engineering, Sun Yat-sen University, Guangzhou 510275, P. R. China.

* Corresponding author: Yuling Hu, Gongke Li

Tel. : +86-20-84110922

Fax : +86-20-84115107

E-mail : ceshyl@mail.sysu.edu.cn

cesgkl@mail.sysu.edu.cn

ABSTRACT: Inspired by the bioadhesive and redox property of marine mussel (3, 4-dihydroxy-phenylalanine (DOPA)), a facile, rapid and economic colorimetric strategy for Hg^{2+} detection was developed. The abundant catechol chains on the surface of Ag@DOPA would reduce Hg^{2+} to Hg^{0} and form Ag@DOPA@Hg nanostructure with the deposition of Hg^{0}. The nanostructure of Ag@DOPA and Ag@DOPA@Hg were demonstrated by X-ray photoelectron spectroscopy, transmission electron microscopy, elemental maps, fourier transform infrared spectrometry. The formation of Ag@DOPA@Hg nanostructure would change the color of Ag@DOPA colloids from golden yellow to purple blue, make it directly detect Hg^{2+} by colorimetric strategy within 5 minutes. With increasing concentrations of Hg^{2+} from 10 nM to 4 μM, the surface plasmon resonance spectral bank of Ag@DOPA colloid decreased and exhibited good linear relationship. The limit of detection was determined as 5 nM. Furthermore, this response was found to be highly selective for Hg^{2+} as the absorption spectra was not affected by other metal ions such as Pb^{2+},Cr^{3+}, Cu^{2+}, Al^{3+}, Ni^{2+}, Co^{2+}, etc. The excellent stability, selectivity and sensitivity of this strategy offer analytical practicability to Hg^{2+} detection in real water samples with recoveries in the range of 104-105% and cosmetic samples with recoveries in the range of 85%-103%.

KEYWORDS: mussel inspired, redox surface, DOPA, colorimetric, core-shell, mercury

INTRODUCTION

3, 4-Dihydroxy-[L-phenylalanine] (DOPA) is the basic composition of Mytilus edulis foot protein 5 (Mefp-5) rich in the adhesive plaque of mussels. The self-polymerization of DOPA and its structural mimic dopamine inspired by mussels is widely used to modify almost any surface with thin and uniform films[1]. The use of DOPA and dopamine functional materials causes a revolution in the surface chemistry and their amazing properties have drawn much attention. For example, some of the fascinating applications include in situ formation of noble metal nanoparticles[2, 3], synthesis of versatile hydrophobic materials[4-6], fabrication of functional "graphene paper"[7] and chelating metal ions to form noble functional materials[8, 9]. In particular, its redox-active catechol group can undergo spontaneous oxidation to quinone under mild solution conditions, thus serving as a reducing agent to form nanoparticles (NPs). DOPA would keep on self-polymerization and coat the newborn NPs with uniform films rich in catechol chains according to its reacting path in melanophore[10, 11]. The catechol chain works like adhesive tentacle for facile functionalization to build a molecular city with its amazing properties. For instance, the biocompatibility and hydrophilicity of the mussel inspired coating make the materials more suitable for biochemical applications such as conjugation of bio-molecules to multi-surface[12, 13], enrichment and detection of bio-molecules[14], bio-imaging[15], etc. On the other hand, the DOPA films full of catechol chains have a redox surface with redox potential about 0.5 V[16], and are so active that can act as reducing agent to reduce metal ions and works as a simple ion sensor.

Hg^{2+} detection has received great attention because of its serious contamination to the environment and toxic damage to human body[17, 18]. The traditional detection methods of Hg^{2+} include atomic absorption spectroscopy, atomic fluorescence spectroscopy, inductively coupled plasma mass spectrometry, but most of them are cost-consuming and procedure-complicated. While other strategies

like colorimetric methods[19-21] are suitable for rapid-detection and cost-saving[18]. Ag or Au nanoparticles were widely used as a colorimetric material for Hg^{2+} detection with its surface plasmon resonance (SPR) signal changing. In order to improve the selectivity and sensitivity for detection of Hg^{2+}, it needs to construct special recognition systems with the modification of Ag or Au nanoparticles. Strategies based on T-Hg^{2+}-T (T represents thymine) structure are widely applied to Hg^{2+} detection because of the high selectivity[22-24]. Hg^{2+} can specially bind to thymine mismatched duplex DNA and form hairpin structure with signal changing. Other strategies are mainly based on the construction of selective chelating binding sites to Hg^{2+} ions[25] or the affinity of Hg^{2+} with sulfur[26, 27]. Most of them are cost-consuming and also needs complicated procedure to construct. There still is strong demand for rapid, cost-effective, and selective methods for the detection of Hg^{2+}.

Inspired of the redox surface of DOPA coating, a one-step, simple and selective colorimetric method has been used for Hg^{2+} detection in this study. DOPA serves as reducing agent for simultaneous producing and modifying Ag NPs with a redox surface constructed by abundant catechol chains. Hg^{2+} is easy to be reduced by the catechol chains and form Ag@DOPA@Hg nanostructure. The formation of Ag@DOPA@Hg would change the SPR signal of Ag@DOPA and cause ~~a~~ color change from golden yellow to purple blue, make it achievable to directly detect Hg^{2+} based on colorimetric strategy. As far as we are aware, this is the first application of the amazing properties of mussel inspired films for colorimetric and visual Hg^{2+} detection.

EXPERIMENTAL SECTION

Reagents and instruments. All of the reagents used in this study were analytical grade. 3, 4-dihydroxy-[L-phenylalanine] (DOPA, 99%) and mercury standard (1000 μg/mL) was purchased from Aladdin industrial corporation (Shanghai, China). Silver nitrate ($AgNO_3$, 99.8%) and other metal salts

were purchased from Guangzhou chemical reagent factory. Borax, $Na_2C_2O_4$, nitric acid and sulfuric acid were purchased from Tianjin chemical reagents factory. UV-Vis spectra were conducted on a CARY 300Conc UV spectrophotometer. The optical photographs were taken by a CASIO EX-ZR300 digital camera. X-ray photoelectron spectroscopic (XPS) analysis was performed on ESCALab250 XPS instrument. Transmission electron microscope (TEM) images and elemental maps were taken by an FEI Tecnai G2 Spirit and FEI Tecnai G2 F30 instruments. Fourier transform infrared (FT-IR) spectra were recorded on a NICOLET AVATAR 330 FT-IR spectrometer.

Synthesis of Ag@DOPA. Ag@DOPA was prepared by reducing $AgNO_3$ in basic aqueous solution with DOPA. Briefly, 0.25 mL DOPA (8 mM) was added to 96 mL basic solution with 400 μM NaOH under the magnetic stirring. Then 3.75 mL $AgNO_3$ (8 mM) was added to the mixed solution and keep stirring for 45 min. The color of the solution changed to gold yellow immediately after the adding of $AgNO_3$ and finally turned to orange red.

Colorimetric detection of Hg^{2+} ions. The detection was performed by adding 25 μL Hg^{2+} ions of certain concentration into 475 μL Ag@DOPA solution and incubated in room-temperature for 5 min. After that, it was ready for spectra analysis.

Analysis of real samples. A water sample was collected locally and was filtered through 0.22 μm membrane, then 250 μM $Na_2C_2O_4$ was added in order to mask the interfering metal ions. A face cream sample was purchased locally and digested by wet reflux digestion method. Briefly, 0.25 g face cream sample was mixed with 15 mL nitric acid, 2.5 mL distilled water and 2.5 mL sulfuric acid respectively. The mixture was refluxed for 2 h and filtered after cooling down at room temperature. The digested liquid was collected and adjusted to neutral before diluted to 50 mL by distilled water. 25 μL of the prepared samples were added to 475 μL Ag@DOPA colloids and incubated in room temperature. After 5 minutes, it was ready for spectra measurement.

Safety considerations. As Hg^{2+} and some of the tested metal ions are highly toxic and have adverse effects to human health and environment, all experiments involving heavy metal ions and other toxic chemicals should be performed with protective gloves. The waste solutions containing heavy metal ions should be collectively reclaimed to avoid polluting the environment.

RESULTS AND DISCUSSION

Mechanism of mussel inspired redox surface for Hg^{2+} detection. The auto-polymerization property of DOPA has drawn more attention due to the widespread applications of mussel inspired films[11, 28]. Scheme 1a illustrates the main reacting path of DOPA in basic aqueous solution. DOPA is easily oxidized to quinone by oxygen in air. DOPA quinone is unstable and would change to 5, 6-dihydroxyindoles by intramolecular cyclization quickly. The mussel inspired films with abundant catechol chains would form via the oxidized polymerization of 5, 6-dihydroxyindoles. The catechol chains of the mussel inspired films are critical for Hg^{2+} detection in this new strategy. As scheme 1b shows, the reduction of Ag^{+} by DOPA would form Ag@DOPA core-shell nanoparticles coated with uniform films (Scheme 1a). As is well-known, the catechol chains are easy oxidized to quinone simultaneously reducing metal ions to metallic form[29, 30]. This property of catechol chains modify the silver colloid with a redox surface that can further reduce Hg^{2+} to Hg^{0} and form a Ag@DOPA@Hg nanostructure without any extra reducing agent. The deposition of Hg^{0} in the shell of Ag@DOPA would change the color of silver colloids from golden yellow to purple blue based on the SPR signal of Ag NPs. Thus, a mussel inspired Ag@DOPA based strategy for Hg^{2+} detection was developed based on the formation of Ag@DOPA@Hg nanostructure, which is different from the reported aggregation strategy based on thymine affinity, coordination effect or sulfur affinity.

Synthesis of Ag@DOPA with redox surface. The in-situ synthesis of Ag@DOPA was performed by simply mixing DOPA with the precursor $AgNO_3$ in basic solution. DOPA is the reductant and stabilizer for the formation of AgNPs. The size of AgNPs increased along with the increasing concentration of DOPA. During the reaction process, the catechol groups lost two protons to form quinone and keep polymerization to coat the newborn Ag NPs with uniform films. The coated films were full of catechol groups that constructed a redox surface for metal ions recognition. As shown in Figure S1a, the characteristic SPR band of the prepared Ag@DOPA NPs was observed in the spectrum at approximately 420 nm. The max absorption value (A_{max}) increased along with the reaction and turned stable within 45 minutes (Figure S1a). At the same time, the pH of the mixture decreased and finally down to about 7.5 because of the releasing protons during the oxidation of catechol groups (Figure S1b). The resulting Ag@DOPA colloids were stable in pH 3-11 and with ionic strength as high as 200 mM NaCl (Figure S1c, d), which indicated its good analytical practicability. The XPS analysis of Ag@DOPA shows the formation of Ag core and the films containing C, N, O elements (Figure S2). The Ag $3d_{5/2}$ peak (Figure 1a) at 367.9 eV corresponding to metallic silver suggests formation of Ag NPs[31]. The C1s spectrum of Ag@DOPA (Figure 1b) comprises three peaks at 284.7, 286.1 and 288.5 eV which can be assigned to C-H, ether or alcoholic and carboxylate group respectively[32]. The peaks at 531.1, 532.7 eV were assigned to carboxylate oxygen and hydroxyl oxygen respectively[32] according to O1s spectrum (Figure 1c). The C1s and O1s XPS spectrum demonstrates the abundant catechol chains on the surface of Ag@DOPA. And a broad peak appeared in 3428 cm^{-1} also indicated the presence of catechol chains according to the FT-IR spectrum of Ag@DOPA (Figure S3). The catechol chain plays an important role to modify the surface of Ag@DOPA with redox property.

Formation of Ag@DOPA@Hg nanoparticles. The redox surface is critical for Hg^{2+} colorimetric detection. The XPS analysis of Ag@DOPA@Hg shows the existence of metallic mercury according to

the characteristic binding energy of mercury at 100.3 eV[31] (Figure 2b), which indicated the successful reduction of Hg^{2+} in the redox surface of Ag@DOPA. And the peak at 101.2 eV belongs to remaining Hg^{2+} ions chelating with O atoms[32] on the surface of Ag@DOPA. The deposition of Hg^0 on the surface of Ag@DOPA would form Hg^0 shell and changed SPR signal of Ag NPs. TEM images of Ag@DOPA (Figure 2c, e) suggested the core-shell structure of Ag NPs reduced by DOPA. In the presence of Hg^{2+}, the catechol chains on the surface of Ag@DOPA would reduce Hg^{2+} to Hg^0 and form Ag@DOPA@Hg NPs with obvious crystalline nature (Figure 2d, f). The HAADF-STEM and elemental mapping of Ag@DOPA (Figure 3) in the presence of Hg^{2+} also show the deposition of Hg^0 on the surface of Ag@DOPA.

In order to identify the importance of the redox surface of Ag@DOPA for Hg^{2+} detection, borax ($Na_2B_4O_7$•10 H_2O) was chosen to be a masking agent for catechol chains. Borax is usually used to protect catechol structure by forming a cyclic bidentate o-benzenediol subunit (Figure 4a)[33]. After the addition of Hg^{2+}, A_{max} decreased and the silver colloids would turned from golden yellow to purple blue (Figure 4b, inset graph) because of the formation of Ag@DOPA@Hg nanostructure. But the addition of borax to Ag@DOPA would mask the catechol chains on the surface, and keep them from reducing Hg^{2+}. There is no color change in the presence of both borax and Hg^{2+} which indicates the successful masking of catechol chains (Figure 4b, inset graph). The influence of borax shows the catechol chains on the surface of Ag@DOPA take a critical part in Hg^{2+} detection.

$Na_2C_2O_4$ is usually used to mask the task metal ion by chelating[2]. However, the addition of $Na_2C_2O_4$ wouldn't influence Hg^{2+} detection, because the chelation between Hg^{2+} and $Na_2C_2O_4$ can't interrupt the reducing of Hg^{2+} by the catechol chain. As Figure 4c shows, the color and the corresponding spectrum did not change after the addition of $Na_2C_2O_4$. The opposite effect of borax and $Na_2C_2O_4$ further supports the mechanism of Hg^{2+} detection is mainly based on the formation of Ag@DOPA@Hg instead of

chelating strategy.

Colorimetric detection of Hg^{2+}. The formation of Ag@DOPA@Hg would change the color of Ag@DOPA colloid, make it directly detect Hg^{2+} with colorimetric methods. The A_{max} of Ag@DOPA decreased after the addition of Hg^{2+} and got stable after reaction for 5 minutes (Figure S3). The color of Ag@DOPA colloids changed immediately after the addition of Hg^{2+} (Figure 5a). ~~a~~And the A_{max} of Ag@DOPA changed linearly with the increasing concentration of Hg^{2+} in the range of 0.01-4 μM (Figure 5b). With the increasing concentration of Hg^{2+}, the A_{max} of Ag@DOPA colloids increased and the calibration curve was A_{max}= -0.1735[Hg^{2+}] + 0.9745(R^2=0.9992). The catechol chains on the surface of Ag@DOPA can also chelate with metal ions[34, 35] such as Cr^{3+}, Pb^{2+}, Cu^{2+} and induce aggregation of Ag@DOPA to interfere Hg^{2+} detection. However, the interference is mainly based on a chelating mechanism that can be broken by adding a stronger chelating ligand than catechol chains. $Na_2C_2O_4$ is a strong bidentate ligand that can chelate with different metal ions and works as a masking agent[2]. The addition of $Na_2C_2O_4$ would avoid the interference by chelating with the interferential metal ions. The selectivity of this method was performed by comparing with over ten kinds of common metal ions with different charges. Cr^{3+}, Al^{3+}, Fe^{3+}, Pb^{2+} and Cu^{2+} would be the mainly interferential ions of Hg^{2+} detection and we used $Na_2C_2O_4$ as masking agent. As Figure 5c, d shows, the addition of Cr^{3+}, Al^{3+}, Fe^{3+}, Pb^{2+} and Cu^{2+} didn't lead to change of color of Ag@DOPA colloids and decrease of absorption value (ΔA represents A_{max} changing after the addition of metal ions) in the presence of $Na_2C_2O_4$. Other test metal ions such as Zn^{2+}, Ni^{2+}, Mn^{2+}, Mg^{2+}, K^+, Na^+ wouldn't interfere even in ten folds of the amount of Hg^{2+} and a hundred folds for K^+ and Na^+ (Figure 5c, d).

The excellent sensitivity and selectivity of this strategy offers the possibility for Hg^{2+} detection in real samples. The detection limit is 5 nM with UV-Vis spectrum measurement which is lower than the toxic level for drinking water regulated by US's EPA. Therefore, we further examined the practicality of this

method for colorimetric detection of Hg^{2+} in river water and face cream samples. A water sample collected from Zhujiang River (Guangzhou, China) was filtered through 0.22 μm membrane and then 250 μM $Na_2C_2O_4$ was added in order to mask the interfering metal ions. Hg^{2+} wasn't detected in the water samples and the spiked-recovery experiment was studied to validate the reliability of this method. The recovery was 105% for 0.050 μM Hg^{2+} and 104% for 2.0 μM Hg^{2+}, indicating good precision of the method. In order to test the feasibility of this method in a more complicated sample, we applied our method to determinate the content of mercury in pharmaceuticals and personal care products (PPCPs). Mercury is well known as an illegal whitening agent used in PPCPs especially in makeup products. The face cream samples were purchased locally and digested by wet reflux digestion method. Hg^{2+} was detected with the concentration of 5.74 mg/g, which was in good agreement with 5.72 mg/g determined by cold vapor atomic absorption spectrometry. When the given amounts of Hg^{2+} were added into face cream samples, the results showed satisfied recoveries in the range of 85%-103%.

CONCLUSION

In summary, we have proposed a new strategy for Hg^{2+} detection based on simultaneous reduction and surface functionalization of silver nanoparticles by mussel-inspired chemistry, followed by the in-situ formation of multilayer Ag@DOPA@Hg core-shell nanostructure. Our method provides a simple and rapid approach to colorimetric detection of Hg^{2+} and shows high selectivity and sensitivity. The investigation of mussel inspired redox surface holds the new trend in surface chemistry based on the amazing properties of DOPA self-polymerization films for interesting applications in noble materials construction, bio-imaging, sensing platforms and others.

ACKNOWLEDGMENT

This work was supported by the National Natural Science Foundation of China (21277176 and 21127008), and by Guangdong Provincial Natural Science Foundation of China under grant number of S2013010012091, respectively.

REFERENCES

1 H. Lee, S. M. Dellatore, W. M. Miller and P. B. Messersmith, *Science*, 2007, **318**, 426.

2 Y. R. Ma, H. Y. Niu, X. L. Zhang and Y. Q. Cai, *Chem. Commun.*, 2011, **47**, 12643.

3 J. A. Jacob, H. S. Mahal, N. Biswas, T. Mukherjee and S. Kapoor, *Langmuir*, 2008, **24**, 528.

4 Q. Zhu and Q. M. Pan, *ACS Nano*, 2014, **8**, 1402.

5 L. Zhang, J. J. Wu, Y. X. Wang, Y. H. Long, N. Zhao and J. Xu, *J. Am. Chem. Soc.*, 2012, **134**, 9879.

6 S. Y. Huang, *ACS Appl. Mater. Interfaces*, 2014, **6**, 17144.

7 J. J. Zhou, B. Duan, Z. Fang, J. B. Song and C. X. Wang, *Adv. Mater.*, 2014, **26**, 701.

8 Q. Liu, N. Y. Wang, J. Caro and A. S. Huang, *J. Am. Chem. Soc.*, 2013, **135**, 17679.

9 P. Y. Sun, J. Wang, X. Yao, Y. Peng, X. X. Tu, P. F. Du, Z. Zheng and X. L. Wang, *ACS Appl. Mater. Interfaces*, 2014, **6**, 12495.

10 S. Ito, *Pigm. Cell Res.*, 2003, **16**, 230.

11 M. d'Ischia, A. Napolitano, A. Pezzella, P. Meredith and T. Sarna, *Angew. Chem., Int. Ed.*, 2009, **48**, 3914.

12 H. Lee, J. Rho, P. B. Messersmith, *Adv. Mater.*, 2009, **21**, 431.

13 Sobocinski, J.; Laure, W.; Taha, M.; Courcot, E.; Chai, F.; Simon, N.; Addad, A.; Martel, B.; Haulon, S.; Woisel, P.; Blanchemain, N.; Lyskawa, J. Mussel Inspired Coating of a Biocompatible Cyclodextrin Based Polymer onto CoCr Vascular Stents. *ACS Appl. Mater. Interfaces*, 2014, **6**, 3575.

14 Y. H. Yan, Z. F. Zheng, C. H. Deng, X. M. Zhang and P. Y. Yang, *Chem. Commun.*, 2013, **49**, 5055.

15 X. Y. Zhang, S. Q. Wang, L. X. Xu, L. Feng, Y. Ji, L. Tao, S. X. Li and Y. Wei, *Nanoscale*, 2012, **4**, 5581.

16 C. Serpentini, C. Gauchet, D. de Montauzon, M. Comtat, J. Ginestar and N. Paillous, *Electrochim. Acta*, 2000, **45**, 1663.

17 E. M. Nolan and S. J. Lippard, *Chem. Rev.*, 2008, **108**, 3443.

18 J. J. Du, L. Jiang, Q. Shao, X. G. Liu, R. S. Marks, J. Ma and X. D. Chen, *Small*, 2013, **9**, 1467.

19 L. Hao, H. Song, Y. Su and Y. Lv, *The Analyst*, 2014, **139**, 764.

20 F. Yang, Q. Ma, W. Yu and X. Su, *Talanta*, 2011, **84**, 411.

21 X. Yuan and Y. Chen, *The Analyst*, 2012, **137**, 4516.

22 X. J. Xue, F. Wang and X. G. Liu, *J. Am. Chem. Soc.*, 2008, **130**, 3244.

23 X. W. Xu, J. Wang, K. Jiao, X. R. Yang, *Biosens. Bioelectron.*, 2009, **24**, 3153.

24 C. W. Liu, Y. T. Hsieh, C. C. Huang, Z. H. Lin and H. T. Chang, *Chem. Commun.*, 2008, 2242.

25 Y. X. Gao, X. Li, Y. L. Li, T. H. Li, Y. Y. Zhao and A. G. Wu, *Chem. Commun.*, 2014, **50**, 6447.

26 F. He, W. Wang, J. W. Moon, J. Howe, E. M. Pierce and L. Y. Liang, *ACS Appl. Mater. Interfaces*, 2012, **4**, 4373.

27 L. Chen, X. L. Fu, W. H. Lu and L. X. Chen, *ACS Appl. Mater. Interfaces*, 2013, **5**, 284.

28 G. Greco, L. Panzella, G. Gentile, M. E. Errico, C. Carfagna, A. Napolitano and M. d'Ischia, *Chem. Commun.*, 2011, **47**, 10308.

29 E. K. Jeon, E. Seo, E. Lee, W. Lee, M. K. Um and B. S. Kim, *Chem Commun (Camb)*, 2013, **49**, 3392.

30 K. Yoosaf, B. I. Ipe, C. H. Suresh and K. G. Thomas, *J. Phys. Chem. C*, 2007, **111**, 12839.

31 E. Sumesh, M. S. Bootharaju, Anshup and T. Pradeep, *J. Hazard. Mater.*, 2011, **189**, 450.

32 S. Kushwaha, B. Sreedhar and P. P. Sudhakar, *Chem. Eng. J.*, 2012, **193-194**, 328.

33 E. Faure, C. Falentin-Daudré, C. Jérôme, J. Lyskawa, D. Fournier, P. Woisel and C. Detrembleur,

Prog. Polym. Sci., 2013, **38**, 236.

34 Y. S. Wu, F. F. Huang, Y. W. Lin, *ACS Appl. Mater. Interfaces*, 2013, **5**, 1503.

35 E. Gaidamauskas, D. C. Crans, H. Parker, K. Saejueng, B. A. Kashemirov, C. E. McKenna, *New J. Chem.*, 2011, **35**, 2877.

FIGURES

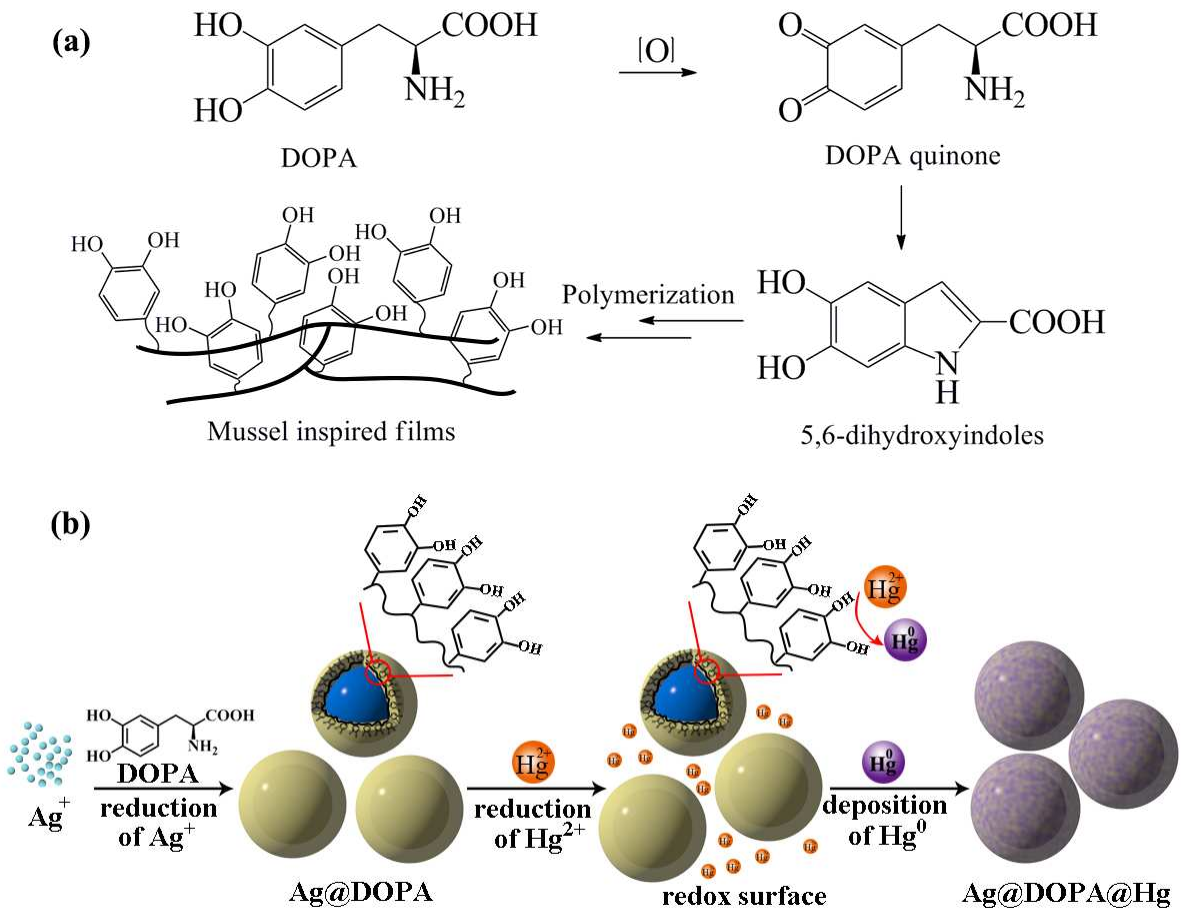

Scheme 1. (a) Schematic outline of DOPA auto-polymerization path; (b) Mechanism of one step colorimetric detection of Hg^{2+}

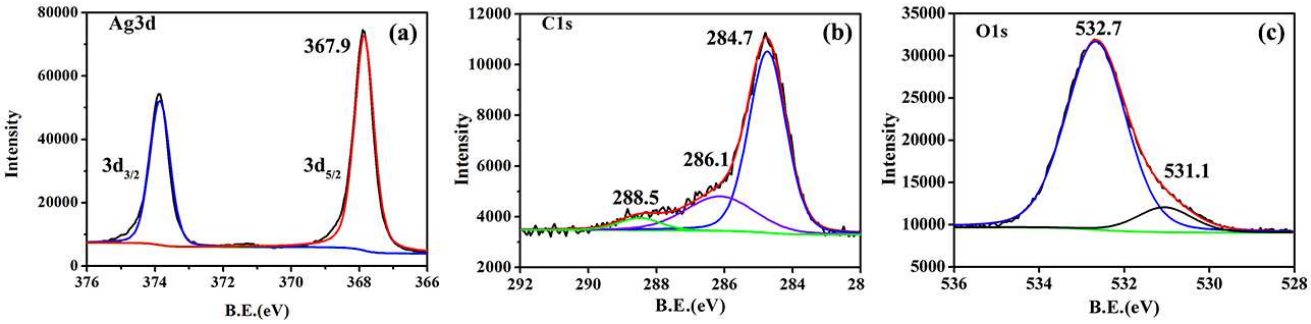

Figure 1. XPS spectra of Ag@DOPA: Ag3d (a), C1s (b), O1s (c).

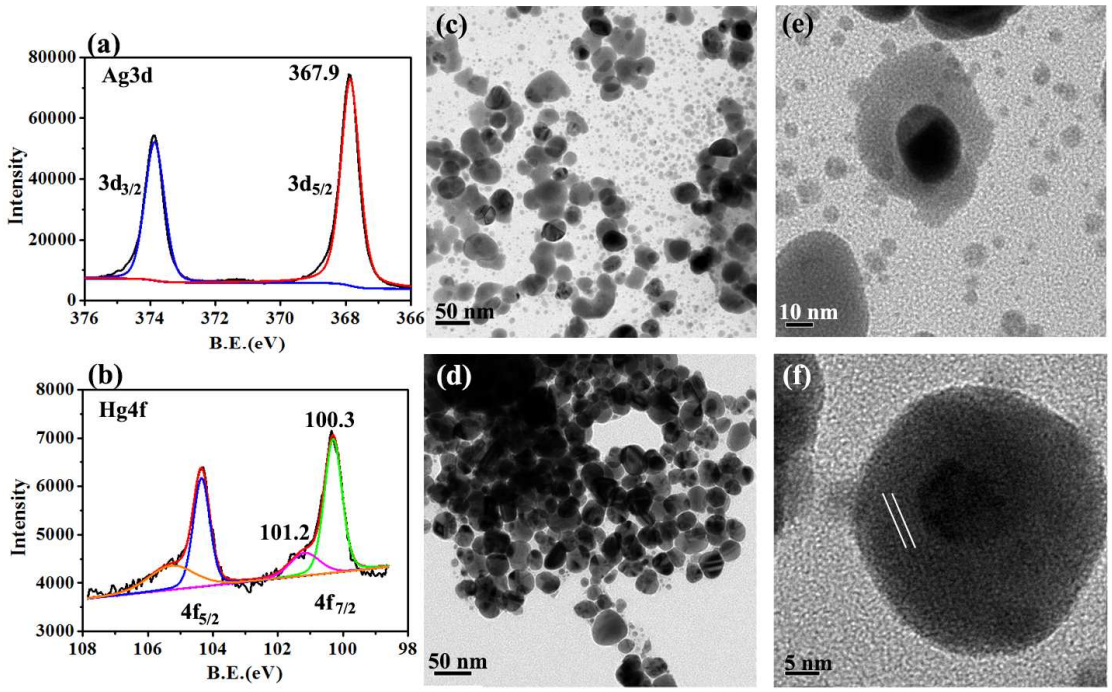

Figure 2. XPS spectra of Ag@DOPA@Hg: Ag3d (a), Hg4f (b); TEM images of Ag@DOPA (c, e) and Ag@DOPA@Hg (d, f). The concentration of Hg^{2+} was 5 μM.

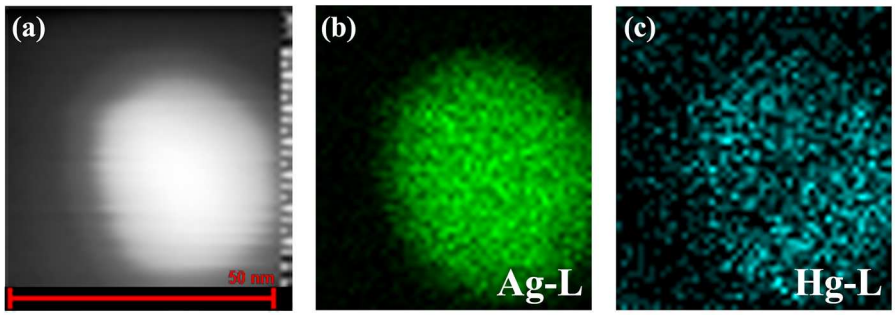

Figure 3. HAADF-STEM (a) and elemental mapping (b, c) of Ag@DOPA@Hg. The concentration of Hg^{2+} was 5 μM.

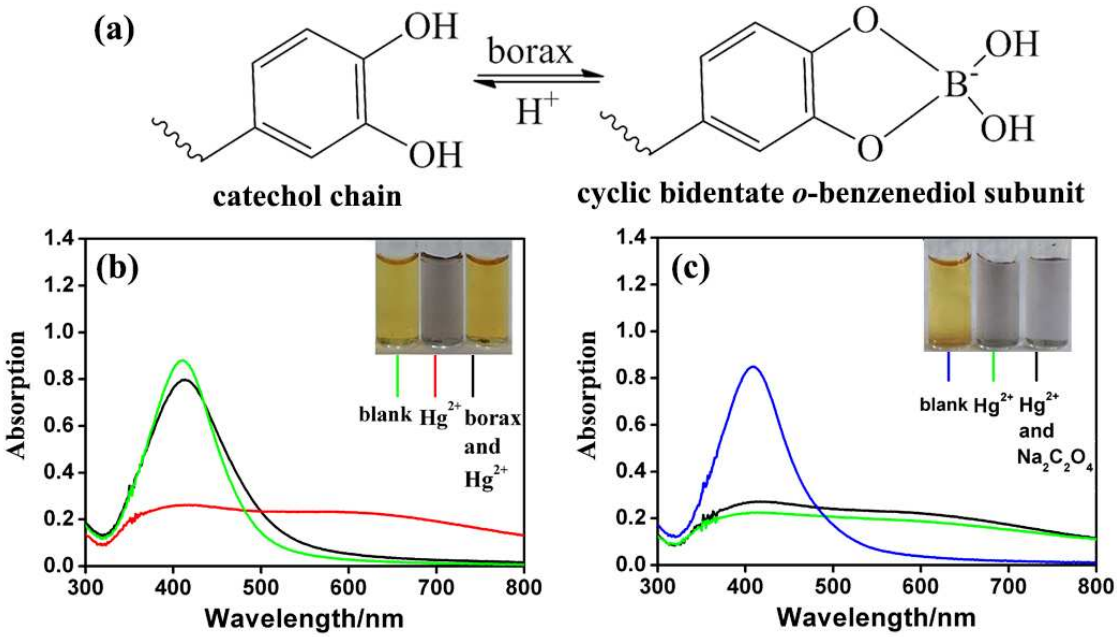

Figure 4. (a) A formula of the formation of cyclic bidentate o-benzenediol subunit; (b) Absorption spectrum of Ag@DOPA: blank, 5 μM Hg^{2+}, 5 μM Hg^{2+} and 5 mM borax; inset graphs are the corresponding photographs; (c) Absorption spectrum of Ag@DOPA: blank, 5 μM Hg^{2+}, 5 μM Hg^{2+} and 250 μM $Na_2C_2O_4$; inset graphs are the corresponding photographs.

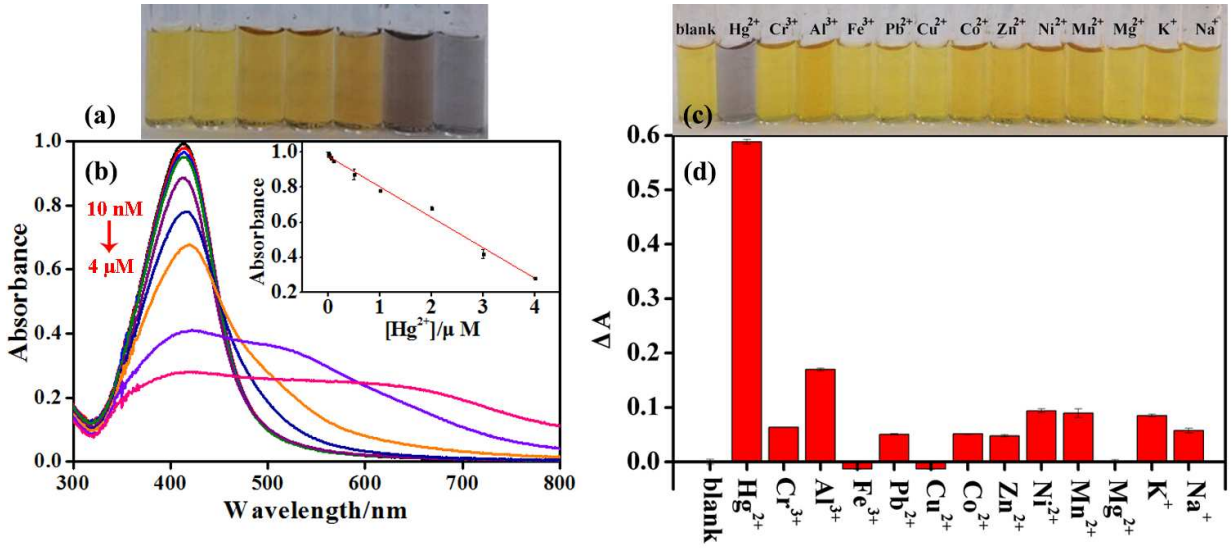

Figure 5. (a) Photographs of Ag@DOPA with different concentration of Hg^{2+}, from left to right: 0 μM; 0.1 μM; 0.5 μM; 1 μM; 2 μM; 3 μM; 4 μM; (b) Absorption spectrum of Ag@DOPA with different Hg^{2+}, from upper to lower: 0 μM; 0.01 μM; 0.05 μM; 0.1 μM; 0.5 μM; 1 μM; 2 μM; 3 μM; 4 μM; inset graph describes the plot of A_{max} against $[Hg^{2+}]$ for mercury analysis. Photographs (c) and ΔA (d) of Ag@DOPA with different kinds of metal ions, from left to right: blank, 5 μM Hg^{2+}; 5 μM Cr^{3+}, Al^{3+}, Fe^{3+}, Pb^{2+} and Cu^{2+} in the presence of 250 μM $Na_2C_2O_4$; 50 μM for Co^{2+}, Zn^{2+}, Ni^{2+}, Mn^{2+}, Mg^{2+}, 500 μM for K^+ and Na^+ without $Na_2C_2O_4$.

Table of Contents (TOC) Image

A facile, rapid and economic colorimetric method for Hg^{2+} detection was designed by formation of Ag@DOPA@Hg nanostructure.